Engineering in Life Sciences

WILEY-VCH

Engineering in Life Sciences

RESEARCH ARTICLE OPEN ACCESS

Downstream Workflows for Intermediate Purification of Lentiviral Vectors Using Tangential Flow Filtration and AEX Membrane Chromatography

Sara Cardoso | Sinan Oender | Jana Engelhardt | Alexander Tappe

Sartorius, Göttingen, Germany

Correspondence: Sara Cardoso (sara.cardoso@sartorius.com)

Received: 15 August 2025 | **Revised:** 19 September 2025 | **Accepted:** 29 September 2025

Funding: The author(s) received no additional funding support for the research, authorship, and/or publication of this article.

Keywords: AEX membrane chromatography | cell and gene therapy | intermediate purification | lentiviral vectors (LVs) | tangential flow filtration (TFF)

ABSTRACT

The growing demand for large quantities of high-purity lentiviral vectors (LVs) has driven the development of scalable, cost-effective purification strategies. Membrane chromatography is particularly well-suited for purifying large biological entities like LVs due to its low mass transfer resistance and minimal back pressure. Among these technologies, anion exchange (AEX) chromatography serves as a key unit operation during the intermediate purification stage of industrial-scale bioprocesses. Sartobind Convec D, a weak AEX membrane with reduced ligand density, lack of hydrogel grafting, and adjusted pore size distribution, was specifically designed for LVs capture. While AEX is commonly employed immediately after clarification to capture LVs, incorporating a tangential flow filtration (TFF) step beforehand can offer several advantages, including product concentration, buffer exchange, and removal of low-molecular-weight impurities. Hydrosart High-Performance TFF membranes, composed of regenerated cellulose, are characterized by high flux rates and are marketed as well-suited for viral vector purification. This study investigated the integration of these two technologies into intermediate purification workflows for LVs. Specifically, the impact of introducing a TFF step prior to AEX chromatography (TFF-AEX workflow) was compared to a process utilizing only AEX chromatography following harvest and clarification (AEX-only workflow). In the AEX-only workflow, Sartobind Convec D membranes were used directly after clarification to capture LVs. These membrane adsorbers can accommodate high flow rates, making them suitable for early downstream processing. In the TFF-AEX workflow, clarified LVs harvests were first concentrated and diafiltrated using Hydrosart TFF membranes, allowing for product enrichment, buffer conductivity adjustment, and removal of smaller contaminants prior to AEX loading. As a result, the TFF-AEX workflow demonstrated improved dynamic binding capacity and enhanced overall impurity removal compared to the AEX-only approach.

1 | Introduction

Lentiviral vectors (LVs) have become essential for modifying patients' cells in and ex vivo due to their ability to deliver large genetic payloads and achieve long-term expression [1, 2]. They are used in several FDA-approved therapies, including CAR-T cell treatments for cancer and therapies like Zynteglo for beta-thalassemia (Approved Cellular and Gene Therapy Products | FDA). These regulatory approvals, along with the growing number of LVs-based clinical trials reported [3] reflect the increasing clinical acceptance and therapeutic potential of LVs. Despite their importance, the supply of high-quality LVs remains a significant barrier to broader adoption of LVs-based therapies and the need for higher yields, increased purity, and improved scal-

ability continue to drive innovation in manufacturing strategies [4–6].

Membrane adsorbers are increasingly replacing traditional resins, offering improved scalability, lower pressure drops, and enhanced cost-efficiency [7, 8]. These chromatography formats rely on convective transport enabling higher flow rates and shorter residence times compared with conventional packed bed resins, which suffer from diffusional limitations and elevated back pressures when processing large viral particles such as LVs [9]. Although initially limited to polishing steps, mainly due to lower binding capacities, newer bind-elute membrane formats have expanded their applicability, matching or even surpassing resins in terms of product quality and cost reduction [10]. The industry predominantly uses AEX for vector capture due to its cost-effectiveness and applicability to LVs pseudotypes [11–13]. Despite its critical role, AEX still presents challenges such as the high conductivities needed for elution and often results in modest functional vector recoveries of around 30%–40% on large-scale processes [13–17]. In literature, these limitations are typically attributed to LVs characteristics, such as complex surface charge distribution and fragile envelope structure and limited understanding of the adsorption mechanisms potentially causing product losses [18]. Recent studies, which have been started to elucidate these mechanisms, have identified specific envelope components responsible for interactions with quaternary-amine membrane adsorbers [19] and that prolonged residence time in the bound state leads to irreversible losses, emphasizing the importance of fast processing [12]. The same group recently highlighted the importance of optimizing membrane properties such as ligand density, pore size, and grafting methods, to improve LVs recovery and facilitate the cost-effective production of viral vectors for gene and cell therapies [6].

Tangential flow filtration (TFF) is an essential operation in LVs purification which is commonly deployed both pre- and post-chromatography, though the sequence is not fully standardized across platforms [16]. This unit operation can complement chromatography by reducing processing volumes, exchanging buffers, and removing small contaminants such as proteins and nucleic acid fragments [4, 13]. Typically, LVs purification involves a limited number of unit operations, with chromatography and TFF as the principal steps to meet drug substance and drug product specifications [20]. Additionally, buffer exchange via TFF ensures conductivity levels compatible with optimal AEX performance [14]. In this regard, flat sheet cassettes can offer great flux performance, improved mixing through turbulence-inducing screens, lower hold-up volumes, and easier scalability. Their widespread use in GMP environments and regulatory familiarity further support their adoption in commercial manufacturing [16, 20]. Given the growing diversity of gene therapy modalities, TFF process optimization is increasingly routine in bioprocess development including technology selection and parameters optimization [21]. Membrane selection depends on both molecular weight cut-off (MWCO) and membrane material. Typical MWCOs range from 100 to 750 kDa, with larger pore sizes improving impurity removal but risking vector loss [13]. Common materials include PES, PVDF, and regenerated cellulose (RC). PES and PVDF offer strong chemical and thermal resistance but can suffer from fouling due to hydrophobicity [22–24]. In contrast, Hydrosart membranes—modified RC—are highly hydrophilic, providing low protein binding, high flux, and robust stability, making them ideal for biopharmaceutical applications [21, 24]. A recent work shows a development strategy for establishing an efficient ultrafiltration and diafiltration (UF|DF) step using Sartocon Hydrosart flat sheet cassettes in LVs purification, technologies geometries, considerations for scale-up compatibility (e.g., pump power constraints) as well as boosting processing times [4]. In the same study, LVs exhibited some tolerance to shear, suggesting that membrane format selection could, in some cases, prioritize process efficiency over traditionally conservative designs. However, as shear sensitivity is not yet fully characterized and may vary with vector design, formulation, and process conditions, operators should proceed with caution—particularly when product integrity is a critical concern [4].

This study evaluates the integration of Sartobind Convec D anion exchanger (AEX) and Hydrosart membranes within intermediate purification workflows for LVs. Two process strategies were compared: (1) an AEX-only workflow, in which AEX chromatography follows immediately after clarification; and (2) a TFF-AEX workflow, which introduces a TFF step prior to chromatography to enable concentration, buffer exchange, and preliminary impurity reduction. By assessing both workflows across key performance indicators—including yield, throughput, and impurity clearance—this study aims to generate practical insights to support the optimization of LVs intermediate purification processes.

2 | Materials and Methods

2.1 | LVs Production

V-SVG lentivirus was produced in suspension within a 10 L Univessel Glass bioreactor, controlled by a Biostat B control tower (Sartorius), through the transient transfection of HEK293 cells using PEIpro (Sartorius). An endonuclease step was performed to digest nucleic acids, optimizing results during downstream processing. The harvest clarification was performed using a Sartopure PP3 20 µm followed by a Sartopure PP3 0.65 µm and Sartoclean 2 0.8 µm (Sartorius) (all size 9 filters). The titer of the LVs material was 1.1×10^8 TU/mL. The clarified LVs were stored in aliquots, frozen at −80°C, and utilized as feed for all subsequent studies.

2.2 | Capture Chromatography (AEX)

LVs harvested clarified material, initially frozen at −80°C, was rapidly thawed (for 5 min) in a 37°C water bath before chromatography. Chromatographic experiments were carried out using a Sartobind Convec D Nano membrane (3 mL volume, 8 mm bed height; Sartorius) on an ÄKTA avant 150 system (Cytiva). Throughout each run, conductivity, UV absorbance at 280 nm, and multiangle light scattering (MALS) signals were continuously monitored. MALS detection (ASTRA Software version 8.2) was performed using a DAWN detector (Waters) to enable real-time analysis of viral particle content. All runs were conducted at a flow rate of 5 membrane volumes per minute (MV/min). The column was equilibrated with a buffer containing 20 mM Tris, pH 7.0. (Buffer A). Elution was carried out using 20 mM

Tris buffer, 10 mM arginine 10 mM $MgCl_2$ supplemented with 1 M NaCl (for the linear gradient) or 2 M (for the step gradient) (Buffer B). Infective capture recovery was calculated comparing the amount of virus in the elution, to the amount initially present in the loading sample. To determine the dynamic binding capacity (DBC), the membrane was loaded with 250 MV of clarified harvest LVs feed diluted in 1:1 in buffer A at a flowrate of 5MV/min (750 mL). The MALS signal was used to track the *break-through* volume profile (C/C0) corresponding to 10%, and the number of loaded particles was measured by p24 concentration.

2.3 | Tangential Flow Filtration (TFF)

LVs harvested clarified material, initially frozen at −80°C, was rapidly thawed (for 5 min) in a 37°C water bath before TFF. TFF was performed using a Sartocon Hydrosart Slice 200 TFF cassette with a pore size of 300 kDa (Sartorius) (effective filter area of 180 cm^2) on the Sartoflow Smart TFF system (Sartorius) by controlling the process through a constant inlet pressure. To identify optimal operating conditions, a permeate flow rate characterization study was conducted at each feed flow rate. For every pump speed, the transmembrane pressure (TMP) was gradually increased until a decline in permeate flux was observed. The optimal TMP was defined as the inflection point preceding this decline. The UF|DF trial was performed using a starting volume of 0.5 L, which corresponded to 28 L/m^2 of membrane surface area. The process consisted of a 10× concentration step, followed by diafiltration with five volumes of exchange buffer (50 mM HEPES, 20 mM $MgCl_2$, 5% sucrose, pH 7.5). After diafiltration, the system and membranes were flushed twice with one hold-up volume (50 mL) each, using recirculated diafiltration buffer for 5 min per flush. These flushes were pooled with the final retentate. Infective LVs recovery was calculated comparing the amount of virus in the retentate after TFF, including flushes, to the amount initially present in the feed.

2.4 | Analytical Methods

2.4.1 | Determination of Infective LVs Titer

The infectious titer of LVs was quantified using live-cell imaging with the Incucyte S3 Live-Cell Analysis System (Sartorius, Germany). HEK293T cells (ACC 635, DSMZ), an adherent cell line, served as the target for transduction. Cells were seeded into suitable culture vessels and exposed to serial dilutions of the LVs preparations. Transduction efficiency was assessed by tracking GFP expression over time. Image capture and analysis were performed in real time using the Incucyte S3 platform. The assay protocol was adapted from the method published by [25], however, compared with the initial procedure, no additional staining was used, and GFP expression was measured 60 h after infection, rather than at the originally specified time point.

2.4.2 | Determination of LVs Particles Titer

LV particle titers were quantified using a p24 enzyme-linked immunosorbent assay (ELISA), performed with the QuickTiter Lentivirus Titer Kit (Cell Biolabs, USA). Absorbance was measured at 450 nm to determine the concentration of the p24 capsid protein in each sample. A second-degree polynomial regression was used to generate the standard curve for quantification. The measured p24 concentrations were then converted to viral particle titers based on the assumption that 1 ng of p24 corresponds to 1.25×10^7 viral particles, with each particle containing approximately 2000 p24 molecules.

2.4.3 | Total dsDNA Quantification

The concentration of total double-stranded DNA (dsDNA) was measured using the Quant-iT Pico-Green dsDNA assay (Thermo Fisher Scientific, USA), following the manufacturer's guidelines. Standards and samples were tested in duplicate using black 96-well microtiter plates (Corning, USA). The samples were excited at a wavelength of 480 nm, and the fluorescence emission intensity was recorded at 520 nm with a FLUOstar Omega plate reader (BMG Labtech, Germany). The standard curve was fitted using linear regression.

2.4.4 | Total Protein Quantification

The total protein concentration was determined using the Pierce Coomassie Bradford protein assay kit (Thermo Fisher Scientific, USA), in accordance with the manufacturer's instructions. Standards and samples were analyzed in duplicate using transparent 96-well microtiter plates (Greiner Bio-One, Austria). The absorbance was measured at 595 nm with a FLUOstar Omega plate reader (BMG Labtech, Germany). A second-degree polynomial was used to fit the standard curve.

3 | Results

AEX chromatography is commonly employed in LVs purification as a core technology for capturing viral particles and reducing impurity levels. This technique operates on the electrostatic attraction between the negatively charged surface of the LVs and the positively charged ligands on the chromatography matrix, typically under neutral pH conditions. In this study, AEX chromatography was evaluated for its effectiveness in capturing LVs within two distinct intermediate purification workflows: one applied immediately after harvest and clarification (AEX-only), and the other following a TFF step used to concentrate the clarified harvest prior to chromatography (TFF-AEX). A schematic overview of the experimental workflows is provided in Figure 1.

3.1 | AEX-Only Workflow

The capture step was performed using the 3 mL Sartobind Convec D Nano, an AEX membrane adsorber, to purify LVs by removing key impurities such as host cell DNA and proteins. Purification was conducted in bind-elute mode, leveraging the electrostatic interaction between the negatively charged viral particles at the working pH and the positively charged ligands of the membrane matrix.

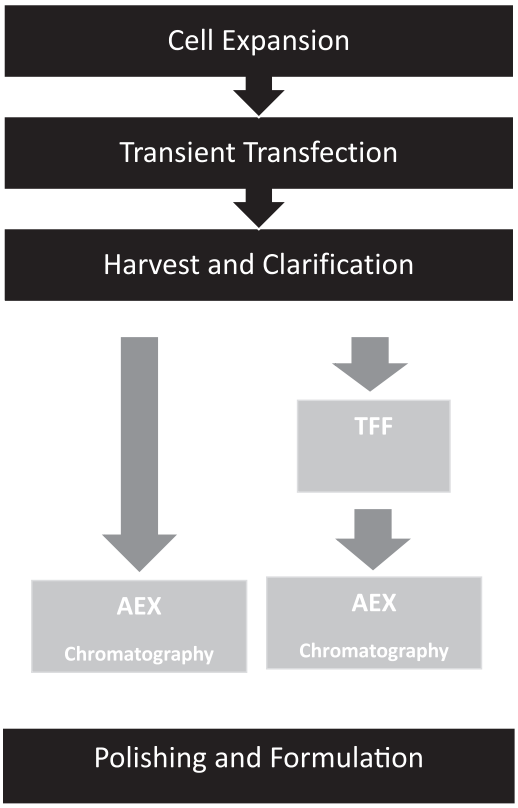

FIGURE 1 | Workflows of the study: AEX-only and TFF-AEX.

3.1.1 | Dynamic Binding Capacity (DBC)

In this study, the appropriate loading range, expressed as the amount of LVs per mL of membrane, was established based on an assessment of the DBC, which is strongly influenced by the quality of the clarified harvest, including viral titer and impurity levels. DBC refers to the amount of viral particles that can be adsorbed per unit volume of the stationary phase under standard operating conditions [8]. Before loading onto the chromatographic membrane, the clarified LVs harvest was diluted in a 1:1 ratio with buffer A to achieve a target conductivity of 7 mS/cm, as determined by preliminary scouting studies. The DBC curve of the Sartobind Convec D membrane was tracked using a multi-angle light scattering (MALS) signal to monitor the DBC at approximately 10% (DBC_{10}) during the loading phase (Figure 2) and the value of loaded particles was assessed by p24 concentration. The DBC profiles exhibited a rapid initial increase, followed by a more gradual progression. Even though a reason for this pattern is not entirely clear, it may be attributed to the LVs being physically retained in some smaller areas of the membrane or from secondary binding effects that slow down membrane saturation after the initial breakthrough [6]. In this case, an approximate DBC_{10} of 1.5E11 particles/mL was obtained (Table 1).

3.1.2 | Capture in Bind Elute Mode

After determining the appropriate lentiviral particles feed loading volume (DBC_{10}), the bind elute chromatography runs were conducted by loading 120 mL of LVs feed (equivalent to 40 membrane volumes, MV) onto the membrane adsorber. Elution was carried out using two strategies, a linear gradient and an isocratic step elution over 40 MV (Table 2). During these chromatographic runs, the LVs were monitored via the MALS signal (Figure 3) and the recovery of infectious particles as well efficiency for removing proteins and DNA removal was assessed (Figure 3, Table 3).

Traditional anion exchangers currently available often require high salt concentrations (up to 1.5–2 M NaCl) to elute the viral

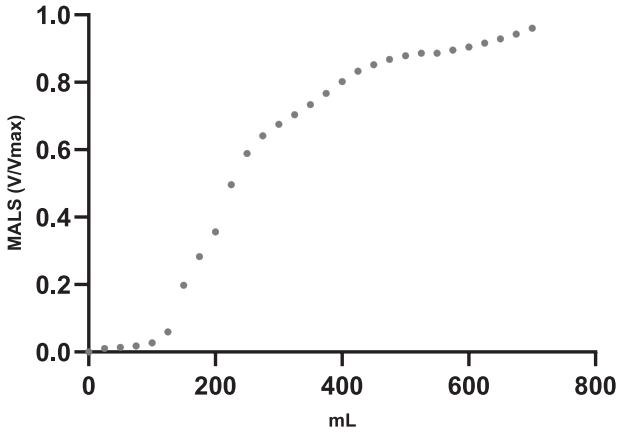

FIGURE 2 | Breakthrough curve profile of harvested clarified LVs using the Sartobind Convec D membrane adsorber. The Multiangle light scattering (MALS) signal (V/V_{max}) was assessed (where Vmax represents the maximum voltage observed at 100% of breakthrough) during loading of the harvested clarified material (mL).

TABLE 1 | Loading volume corresponding to 10% of *breakthrough* (BT_{10}) and respective DBC_{10} (particles/mL membrane) for harvested clarified LVs using Sartobind Convec D chromatographic membrane adsorber.

Sartobind Convec D Nano 3 mL	
Volume BT_{10} (mL)	120
DBC_{10} (particles/mL membrane)	1.53E+11

TABLE 2 | Chromatographic elution modes applied to the Sartobind Convec D chromatographic membrane adsorber to recover LVs.

Elution mode	**Load (MV) (7–10 mS/cm)**	**NaCl (M)**	**Conductivity MPB (mS/cm)**
Linear gradient	40	0–2	92–158
Step gradient	40	1	92

TABLE 3 | Overview of infective recovery (%), protein and DNA removal ranges (%) obtained by processing clarified LVs using Sartobind Convec D chromatographic membrane adsorber.

Sartobind Convec D Nano	
Infective recovery (%)	65–74
Protein removal (%)	85–90
DNA removal (%)	30–60

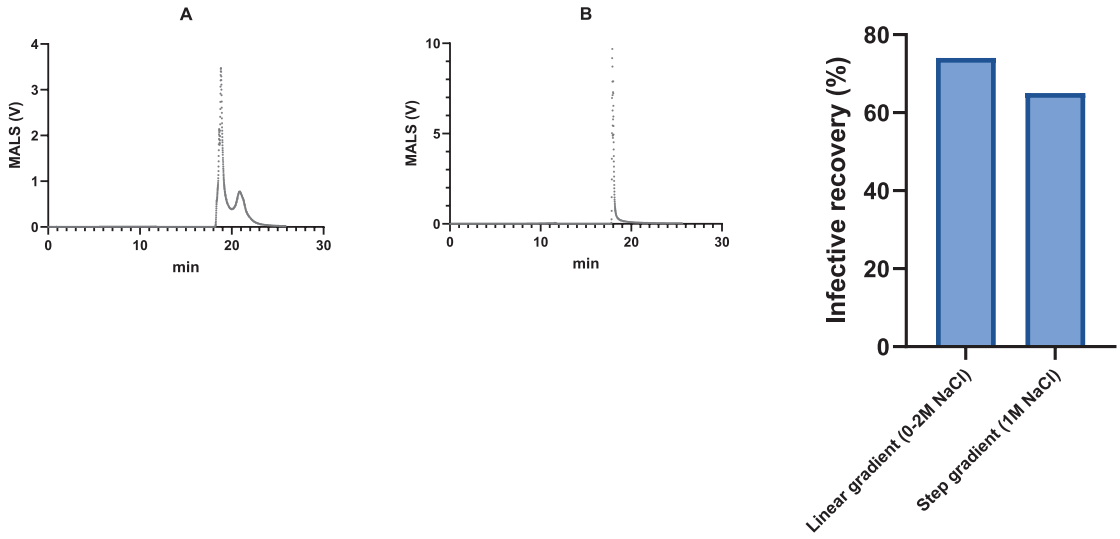

FIGURE 3 | Multiangle light scattering (MALS) signal (V) for the LVs using two different elution modes (A: linear gradient; B: step gradient) and infective recovery (%) by processing harvested clarified LVs using Sartobind Convec D chromatographic membrane adsorber.

particles exhibiting very broad and heterogenous elution profiles, while often providing only poor recoveries on larger scales [13, 15, 16]. In fact, this complicates effective vector purification, as eluting at high salt concentrations can compromise vector functionality, and broad elution profiles often lead to co-elution of residual host cell DNA (hcDNA) and plasmid DNA (pDNA) along with the vector. Due to the reported sensitivity of LVs to salt, a key process advantage is the ability to elute LVs efficiently at low salt concentrations (A.S. Moreira et al., 2021). Strategies have been reported to overcome the salt sensitivity, such as the use of weak DEAE ligands due to their low salt elution requirements [26], diluting the eluate into a low-salt buffer immediately after elution to prevent material loss and the use of stabilizers like non-reducing sugars, polyols, and proteins have been shown to enhance LVs stability [27]. From this perspective, Sartobind Convec D showed strong compatibility with the enveloped, infectious LVs under both gradient and isocratic elution modes, achieving good peak profiles during elution of the lentiviral particles at relatively low conductivity ranges (Figure 3, Table 3). Examining the run using a gradient elution, the MALS signal reveals a broad "two-peak" profile in the chromatogram (Figure 3). Separate LVs populations with inherent structural differences are described in the literature, which show different binding species on their envelope, have been reported as potential causes of the individual peak elution [12, 19]. However, the same phenomenon is not observed when an isocratic elution is applied, where a single sharp peak is observed (Figure 3). Even though the linear gradient approach slightly improved recovery of infective lentiviral particles (74%) compared to isocratic elution with 1 M (65%), one could argue that it may be influenced by the reduced salt exposure in the gradient method, as in this case the total of LVs were recovered with less than 750 mM NaCl. In fact, most LVs (70%–80%) are eluted below 400 mM NaCl and this is likely due to weaker interactions between the virus particles and the chromatography ligands of Sartobind Convec D. Another key process point, the lower ligand density offered by Sartobind Convec D reduces virus-ligand interaction, resulting in a significant benefit as it reduces the need for salt addition to the feed to weaken electrostatic interactions during loading. Lastly, as AEX relies on electrostatic interactions, it typically lacks selectivity for LVs, binding not only viruses but also negatively charged nucleic acids and proteins. Sartobind Convec D proved highly effective at removing proteins during the loading phase, with 85%–90% of total protein cleared in the flowthrough while the viral particles were retained. This efficient host cell protein clearance preserved binding capacity for viral particles. DNA removal was less efficient, with residual DNA clearance ranging from 30% to 60%, resulting in partial co-elution of residual DNA (Table 3).

3.2 | TFF-AEX Workflow

The ultrafiltration and diafiltration (UF|DF) step was performed using the Sartocon Hydrosart Slice 200, 300 kDa TFF cassette to concentrate and diafiltrate LVs from the harvested clarified feed. This process enabled the removal of small impurities such as host cell proteins and DNA fragments. Following TFF, the concentrated and diafiltrated LVs feed was processed using the 3 mL Sartobind Convec D Nano membrane adsorber using AEX chromatography.

3.2.1 | Tangential Flow Filtration

The optimal TFF parameters, such as TMP and Δ Pressure (ΔP) for the intended crossflow rate, were previously established for the LVs feed stream in another study [4] and applied to the ultrafiltration and diafiltration process (Table 4). The performance of the TFF step was further evaluated based on the recovery of infectious particles and the removal efficiency of host cell proteins and residual DNA (Figure 4).

During processing, the TMP was maintained between 0.50 and 0.60 bar, with a set ΔP of 0.80 bar. Under these optimized conditions, near-complete recovery of infectious lentiviral particles (~100%) was achieved, along with substantial impurity reduction -63% protein removal and 45% DNA removal (Figure 4).

TABLE 4 | Parameters used for the ultrafiltration and diafiltration of harvested clarified LVs using a Sartocon Hydrosart 300 kDa TFF cassette.

Sartocon Hydrosart 300 kDa	
Inlet Pressure (fixed) (bar)	0.95
Δ Pressure (ΔP) (bar)	0.80
TMP (bar)	0.55
Target UF | DF (fold)	10x | 5x

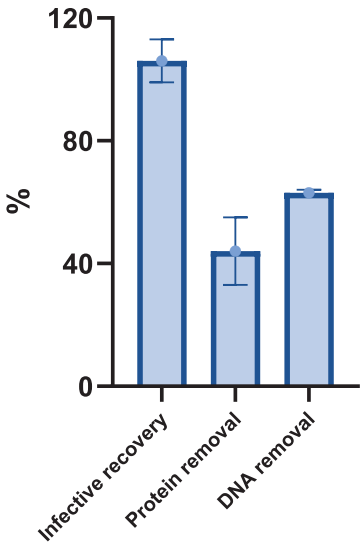

FIGURE 4 | Overview of infective recovery (%), protein and DNA removal (%) obtained by processing harvested clarified LVs using using Sartocon Hydrosart 300 kDa TFF cassette (mean ± SD; $n = 2$).

TABLE 5 | Loading volume corresponding to 10% *breakthrough* (BT_{10}) and respective DBC_{10} (particles/mL membrane) for ultrafiltrated and diafiltrated LVSs using Sartobind Convec D chromatographic membrane adsorber.

Sartobind Convec D Nano	
Volume BT_{10} (mL)	25
DBC_{10} (particles/mL membrane)	6.2E+11

3.2.2 | AEX Chromatography

3.2.2.1 | Dynamic Binding Capacity. As per the AEX-only workflow, the TFF-AEX workflow required determination of an appropriate loading range, expressed as the amount of LVs per mL of membrane, based on the DBC of the processed material (Table 5). However, unlike the AEX-only approach, the retentate obtained from the TFF step was directly loaded onto the chromatographic membrane without additional buffer conductivity adjustment.

3.2.2.2 | Capture in Bind Elute mode. Following the determination of the appropriate LVs feed loading volume (DBC_{10}), bind-elute chromatography was performed by loading 25 mL of the harvested clarified ultrafiltrated and diafiltrated LVs (equivalent to 8 membrane volumes, MV), onto the membrane adsorber.

TABLE 6 | Overview of infective recovery, protein and DNA removal (%) obtained by processing harvested clarified ultrafiltrated and diafiltrated LVs using Sartobind Convec D chromatographic membrane adsorber.

Sartobind Convec D Nano	
Infective recovery (%)	60
Protein removal (%)	*Below limit of detection (LOD)*
DNA removal (%)	49

Elution was performed using the same linear gradient mode strategy applied before over 40 MV. Lentiviral particles were monitored throughout the chromatographic run using a MALS and the recovery of infectious particles as well efficiency for removing proteins and DNA removal was accessed (Table 6).

In this step, processing of the harvested clarified ultrafiltrated and diafiltrated LVs feed resulted in an infective virus particle recovery in the same range as obtained when the membrane adsorber is used to capture LVs directly from the harvested clarified feed (approximately 60%). Regarding contaminants' profile, no detectable protein contamination was observed (considering the limit of detection of the assay) and approximately 49% of residual DNA was removed during the capture step.

3.3 | AEX-Only Versus TFF-AEX Workflow

Harvested clarified LVs solutions often exhibit high conductivity, which can impair the performance of AEX chromatography systems. These systems are known to be sensitive to elevated conductivity levels [13, 14, 16]. One approach to mitigate this challenge, here referred to as the AEX-only workflow, involves diluting the LVs feed with a chromatography-compatible buffer to reduce conductivity to acceptable levels. However, this strategy significantly increases the process volume. At larger manufacturing scales, this increase in volume necessitates larger chromatography matrices. In such cases, membrane adsorbers—offering high flow rate capabilities—are advantageous, particularly in early process stages where high-throughput is essential.

In contrast, the TFF-AEX workflow integrates TFF prior to AEX chromatography. This approach enables conductivity reduction via diafiltration, eliminating the need for dilution and preserving LVs concentration. Simultaneously, the LVs feed is concentrated, resulting in a substantial reduction—approximately five-fold—in both the volume and duration of the subsequent chromatography step (Table 7, Figure 5). Optimal selection of TFF cassettes and process parameters allowed high recovery of infective LVs, with no compromise in yield (Figure 5).

Moreover, TFF effectively removes small molecular weight impurities such as host cell proteins and fragmented DNA, which can otherwise compete with LVs for membrane binding during AEX. This enhanced pre-chromatography purification improves the performance of the membrane adsorber. In particular, Sartobind Convec D membranes demonstrated efficient protein clearance

TABLE 7 | Comparison of loading volume (mL), loading time (min), DBC_{10} (particles/mL) as well as infective recovery (%), protein and DNA removal (%) obtained by using AEX-only and TFF-AEX intermediate workflows to process LVs.

	AEX-Only	TFF-AEX
Loaded volume (mL)	120	25
Loading time (min)	24	5
DBC_{10} (particles/mL membrane)	1.5E+11	6.2E+11
Infective recovery (%)	65-74	60
Protein removal (%)	85-90	~100
DNA removal (%)	30-60	81

during loading, contributing to an observed four-fold increase in DBC -6.2 × 10^{11} particles/mL membrane—under the TFF-AEX workflow (Table 7). This increased binding efficiency allows for the use of smaller chromatography devices at manufacturing scale, contributing to a more economical and scalable process. Besides, both the AEX-only and TFF-AEX workflows consistently achieved high infective LVs recoveries (≥60%) when using Sartobind Convec D membranes.

Despite its advantages, TFF alone is limited in its ability to remove large DNA species such as genomic DNA and histone complexes. Therefore, a DNase digestion step is often employed upstream of TFF to fragment genomic DNA and enhance its removal during AEX chromatography [14, 20]. Higher amounts of residual DNA were detected in the drug substance produced using the AEX-only workflow (104 ng/mL) compared to the TFF-AEX workflow (27 ng/mL). Generally, it is advised to limit residual DNA to less than 10 ng per dose [28]. Assuming a dose of 1 × 10^9 TU, the AEX-only process results in a 1.2-fold decrease in DNA mass per dose (from 2.7 to 2.3 μg), whereas the TFF-AEX process achieves a 3.7-fold decrease (from 5.4 to 1.4 μg). It is important to highlight that these figures are for processes comparison only and do not represent the final administered amounts, as additional downstream processing is performed to prepare the final formulated LVs drug product.

Lastly, it is important to consider the influence of viral particles concentration on binding interactions. At higher concentrations, LVs may undergo a transition from reversible to irreversible binding due to strong attractive forces and multipoint attachment to membrane surfaces. A recent study demonstrated that increased membrane loading can mitigate this effect by saturating available binding sites, thereby reducing the incidence of irreversible interactions [6]. From this perspective, the TFF-AEX

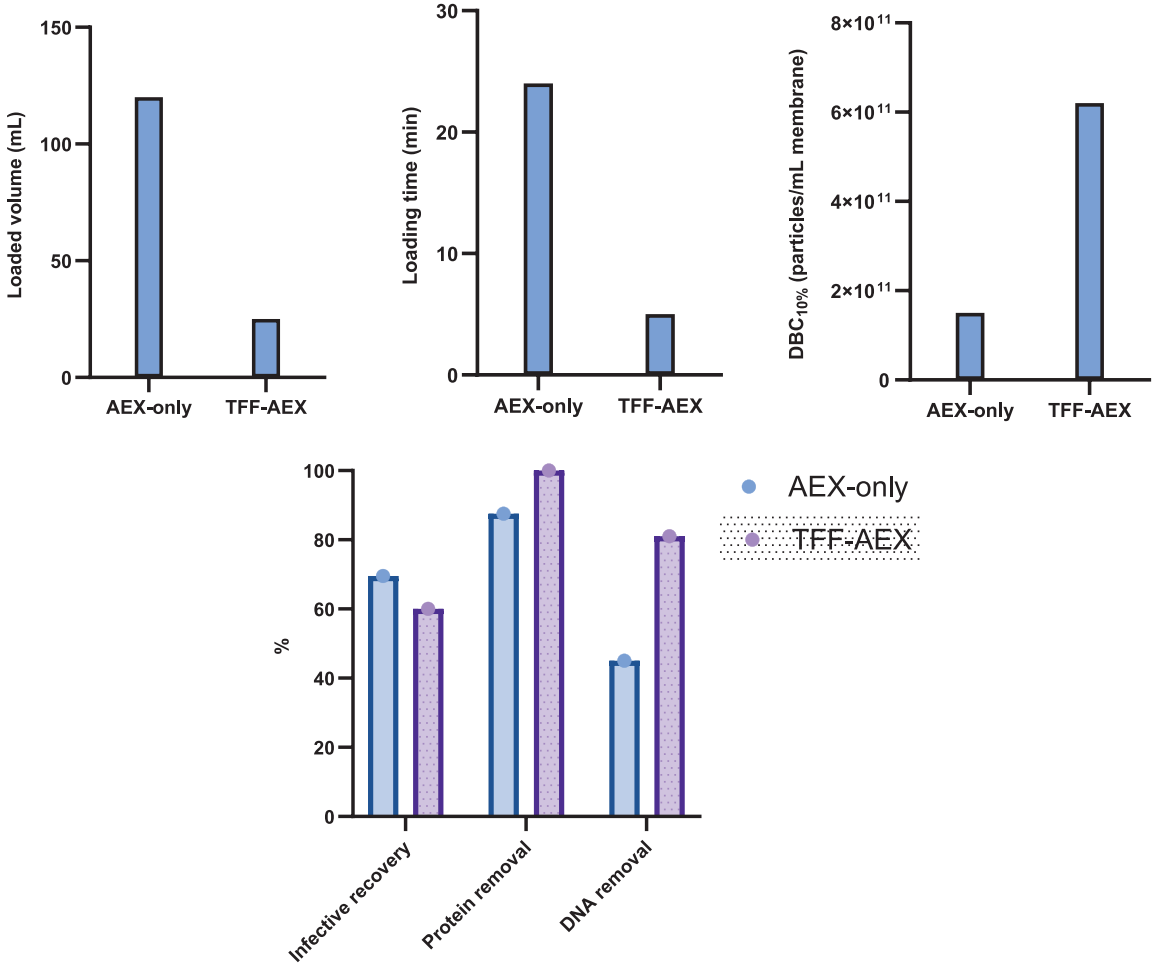

FIGURE 5 | Overview of loading volume (mL), loading time (min), $DBC_{10\%}$ (particles/mL) as well as infective recovery (%), protein and DNA removal (%) obtained by using AEX-only and TFF-AEX intermediate workflows to process LVs.

process enables the use of more concentrated LVs feedstreams, potentially enhancing chromatographic performance and process robustness.

4 | Conclusion

The primary goal of the study was to compare the effectiveness of two purification workflows for intermediate LVs purification, focusing on the use of AEX chromatography and TFF unit operations: AEX-only and TFF-AEX workflow. In the first case, AEX chromatography was applied directly after clarification without the intermediate TFF step. Convective-based matrices like Sartobind Convec D membrane adsorbers have proven to be highly beneficial to handle large flow rates, making them suitable for early processing stages. In the second workflow, TFF was applied before AEX chromatography to concentrate the viral product, thereby reducing viral feed stream volumes for AEX chromatography, and to remove smaller impurities, which enhances dynamic binding capacities. Besides, employing TFF prior AEX chromatography, was useful to achieve lower conductivities without sample dilution before chromatography. This resulted in reduced loading times by five-fold to load an increased particles number by three to four times higher using the same membrane adsorber volume. Overall, excellent recovery could be achieved during the ultrafiltration and diafiltration step using Sartocon Hydrosart Slice 200 TFF cassette, when selecting the right pore size and process parameters.

Both unit operations faced difficulties in removing larger DNA molecules, therefore combining AEX chromatography and/or TFF with strategies to clear DNA impurities, like a DNAse digestion, is a must in LVs purification processes. Incorporating a TFF step prior to AEX chromatography results in incremental contaminant reduction without significant product loss when operated under optimal conditions. This translates to higher dynamic binding capacities for virus particles using the same membrane adsorber volume, thereby allowing for a significant downsizing of the necessary adsorber in a manufacturing process scale.

In conclusion, chromatography remains central to LVs purification, with membrane-based AEX platforms offering a promising path forward leading to significantly improve throughput and reduce membrane usage at manufacturing scale. This study has demonstrated that combining TFF and membrane-based AEX chromatography can enhance overall process efficiency, by reducing the volume and conductivity of the feed stream, which improves virus binding capacity on AEX membranes and reduces processing time. However, even with these advancements, complete DNA clearance often requires additional steps, such as enzymatic digestion.

Acknowledgments

The authors would like to thank Katja Heinrichs for the analytics execution support, Dr. Magda Tomala and Dr. Suneetha Nunna for viral feed stream production, Dr. Axel Thiefes and Lucas Herbst for harvest and clarification processing.

Conflicts of Interest

The authors Sara Cardoso, Sinan Oender, Jana Engelhardt, and Alexander Tappe declare no conflicts of interest.

Data Availability Statement

The data that support the findings of this study are available from the corresponding author upn reasonable request.

References

1. J. T. Bulcha, Y. Wang, H. Ma, P. W. L. Tai, and G. Gao, "Viral Vector Platforms Within the Gene Therapy Landscape," *Signal Transduction and Targeted Therapy* 6, no. 1 (2021):53, https://doi.org/10.1038/s41392-021-00487-6.

2. D. J. Stibbs, P. Silva Couto, Y. Takeuchi, Q. A. Rafiq, N. B. Jackson, and A. C. M. E. Rayat, "Continuous Manufacturing of Lentiviral Vectors Using a Stable Producer Cell Line in a Fixed-Bed Bioreactor," *Molecular Therapy—Methods & Clinical Development* 32, no. 1 (2024): 101209, https://doi.org/10.1016/j.omtm.2024.101209.

3. S. L. Ginn, M. Mandwie, I. E. Alexander, M. Edelstain, and M. R. Abedi, "Gene Therapy Clinical Trials Worldwide to 2023—An Update," *Journal of Gene Medicine* 26, no. 8 (2024): e3721.

4. S. Cardoso, S. Krueger, J. Engelhardt, and A. Tappe, "Development of a Robust Large Scale Downstream Processing of Lentiviral Vectors Using Tangential Flow Filtration," *Separation and Purification Technology* 378, no. 1 (2025):134568, https://doi.org/10.1016/j.seppur.2025.134568.

5. J. J. Labisch, M. Evangelopoulou, T. Schleuß, and A. Pickl, "Investigating Ultrafiltration Membranes and Operation Modes for Improved Lentiviral Vector Processing," *Engineering in Life Sciences* 25, no. 1 (2025):e202400057, https://doi.org/10.1002/elsc.202400057.

6. G. Pamenter, D. H. Rahim, C. Lamont, M. Kapanidou, K. Pemberton, R. Sanches, A. Kulkarni, O. Goodyear, C. Knevelman, K. Mitrophanous, A. Krause, F. Taft, V. Thom, D. G. Bracewell, and L. Davies, "Membrane Adsorber Design for Lentiviral Vector Recovery," *Molecular Therapy — Methods & Clinical Development* (2025): 101533, https://doi.org/10.1016/j.omtm.2025.101533.

7. K. Lothert and M. W. Wolff, "Affinity and Pseudo-Affinity Membrane Chromatography for Viral Vector and Vaccine Purifications: A Review," *Membranes* 13, no. 9 (2023): 70, https://doi.org/10.3390/membranes13090770.

8. Y. Qu, I. Bekard, B. Hunt, et al., "The Transition From Resin Chromatography to Membrane Adsorbers for Protein Separations at Industrial Scale," *Separation* 53, no. 4 (2023): 351–371, https://doi.org/10.1080/15422119.2023.2226128.

9. A. Schimek, J. K. M. Ng, F. Rischawy, and J. Hubbuch, *Mechanistic Modeling of the Elution Behavior and Convective Entrapment of Vesicular Stomatitis Virus (vsv) on an Ion Exchange (iex) Chromatography Monolith* (Elsevier BV, 2025), https://doi.org/10.2139/ssrn.5101563.

10. Z. Dabaghian, E. Pakkaner, L. Kong, and X. Yang, "A Review on Chromatographic Membranes for Antibody Purification: Factors Affecting Binding Capacity and Guidelines for Membrane Design," *Separation and Purification Technology* 357 (2025): 130147, https://doi.org/10.1016/j.seppur.2024.130147.

11. P. Nestola, C. Peixoto, R. R. J. S. SiLVsa, P. M. ALVses, J. P. B. Mota, and M. J. T. Carrondo, "Improved Virus Purification Processes for Vaccines and Gene Therapy," *Biotechnology and Bioengineering* 112, no. 5 (2015): 843–857, https://doi.org/10.1002/bit.25545.

12. G. Pamenter, L. Davies, C. Knevelman, et al., "Time-Dependent Sorption Behavior of Lentiviral Vectors During Anion-Exchange Chromatography," *Biotechnology and Bioengineering* 120, no. 8 (2023): 2269–2282, https://doi.org/10.1002/bit.28483.

13. A. J. Valkama, I. Oruetxebarria, E. M. Lipponen, et al., "Development of Large-Scale Downstream Processing for Lentiviral Vectors," *Molecular*

Therapy—Methods & Clinical Development 17 (2020): 717–730, https://doi.org/10.1016/j.omtm.2020.03.025.

14. V. S. Bandeira, C. Peixoto, A. F. Rodrigues, et al., "Downstream Processing of Lentiviral Vectors: Releasing Bottlenecks," *Human Gene Therapy Methods* 23 (2012): 255–263, https://doi.org/10.1089/hum.2012.059. 121017063203000.

15. R. Ghosh, S. Koley, S. Gopal, A. L. Rodrigues, J. S. Dordick, and S. M. Cramer, "Evaluation of Lentiviral Vector Stability and Development of Ion Exchange Purification Processes," *Biotechnology Progress* 38, no. 6 (2022), https://doi.org/10.1002/btpr.3286.

16. A. S. Moreira, D. G. Cavaco, T. Q. Faria, P. M. Alves, M. J. T. Carrondo, and C. Peixoto, "Advances in Lentivirus Purification," *Biotechnology Journal* 16, no. 1 (2020):e2000019, https://doi.org/10.1002/biot.202000019.

17. J. Ruscic, C. Perry, T. Mukhopadhyay, Y. Takeuchi, and D. G. Bracewell, "Lentiviral Vector Purification Using Nanofiber Ion-Exchange Chromatography," *Molecular Therapy—Methods & Clinical Development* 15 (2019): 52–62, https://doi.org/10.1016/j.omtm.2019.08.007.

18. A. McCarron, M. Donnelley, C. McIntyre, and D. Parsons, "Challenges of Up-Scaling Lentivirus Production and Processing," *Journal of Biotechnology* 240 (2016): 23–30, https://doi.org/10.1016/j.jbiotec.2016.10.016.

19. G. Pamenter, L. Davies, C. Lamont, et al., "Lentiviral Vector Determinants of Anion-Exchange Chromatography Elution Heterogeneity," *Biotechnology and Bioengineering* 121, no. 9 (2024): 2936–2951, https://doi.org/10.1002/bit.28766.

20. C. Perry and A. C. M. E. Rayat, "Lentiviral Vector Bioprocessing," *Viruses* 13, no. 2 (2021): 268, https://doi.org/10.3390/v13020268.

21. S. Mendes, T. Q. Faria, A. Nascimento, et al., "Accelerated Development of AAV Purification Process Using a High-Throughput and Automated Crossflow System," *Separations* 11, no. 3 (2024): 73, https://doi.org/10.3390/separations11030073.

22. B. Keskin, T. Ormancı-Acar, T. Türken, D. Y. Imer, and I. Koyuncu, "Effect of Wetting Agent onthe Dye Filtration Performance of Ultrafiltration Membrane," *Water Science & Technology* 82, no. 3 (2020): 577–586, https://doi.org/10.2166/wst.2020.364.

23. E. Madsen, J. Kaiser, U. Krühne, and M. Pinelo, "Single Pass Tangential Flow Filtration: Critical Operational Variables, Fouling, and Main Current Applications," *Separation and Purification Technology* 291 (2022): 120949, https://doi.org/10.1016/j.seppur.2022.120949.

24. A. L. Zydney, "New Developments in Membranes for Bioprocessing—A Review," *Journal of Membrane Science* 620 (2021): 118804, https://doi.org/10.1016/j.memsci.2020.118804.

25. J. J. Labisch, G. P. Wiese, K. Barnes, F. Bollmann, and K. Pflanz, "Infectious Titer Determination of Lentiviral Vectors Using a Temporal Immunological Real-Time Imaging Approach," *PLoS One* 16, no. 7 (2021): e0254739, https://doi.org/10.1371/journal.pone.0254739.

26. D. Boudeffa, B. Bertin, A. Biek, et al., "Toward a Scalable Purification Protocol of gaLVs-tr-Pseudotyped Lentiviral Vectors," *Human Gene Therapy Methods* 30, no. 5 (2019): 153–171, https://doi.org/10.1089/hgtb.2019.076.

27. M. Carmo, A. Alves, A. F. Rodrigues, et al., "Stabilization of Gammaretroviral and Lentiviral Vectors: From Production to Gene Transfer," *Journal of Gene Medicine* 11, no. 8 (2009): 670–678, https://doi.org/10.1002/jgm.1353.

28. H. Yang, "Establishing Acceptable Limits of Residual DNA," *PDA Journal of Pharmaceutical Science and Technology* 67, no. 2 (2013): 155–163, https://doi.org/10.5731/pdajpst.2013.00910.